

Finite low-temperature entropy of some strongly frustrated quantum spin lattices in the vicinity of the saturation field

Oleg Derzhko^{1*} and Johannes Richter^{1†}

¹Max-Planck-Institut für Physik komplexer Systeme, Nöthnitzer Straße 38, 01187 Dresden, Germany

(Dated: February 2, 2008)

For a class of highly frustrated antiferromagnetic quantum spin lattices the ground state exhibits a huge degeneracy in high magnetic fields due to the existence of localized magnon states. For some of these spin lattices (in particular, the 1D dimer-plaquette, sawtooth and kagomé-like chains as well as the 2D kagomé lattice) we calculate rigorously the ground-state entropy at the saturation field. We find that the ground-state entropy per site remains finite at saturation. This residual ground-state entropy produces a maximum in the field dependence of the isothermal entropy at low temperatures. By numerical calculation of the field dependence of the low-temperature entropy for the sawtooth chain we find that the enhancement of isothermal entropy is robust against small deviations in exchange constants. Moreover, the effect is most pronounced in the extreme quantum case of spin $\frac{1}{2}$.

PACS numbers: 75.10.Jm, 75.45.+j

Keywords: frustrated antiferromagnets, localized magnons, ground-state entropy

Antiferromagnetically interacting quantum spin systems on geometrically frustrated lattices have attracted much attention during the last years^{1,2,3}. Whereas in general frustration makes the eigenstates of the quantum spin system very complicated, it has been found recently that in the vicinity of the saturation field for a wide class of frustrated spin lattices just owing to frustration the ground states become quite simple. These exact ground states consist of independent localized magnons in a ferromagnetic environment^{3,4,5}. They lead to a macroscopic jump in the zero-temperature magnetisation curve just below saturation^{3,4,5} and may provide instabilities towards lattice deformations⁶.

In the present paper we examine the low-temperature entropy of several highly frustrated antiferromagnetic spin lattices which may host independent localized magnons in the vicinity of the saturation field. The ground state of such a system at saturation exhibits a huge degeneracy which grows exponentially with system size. For some of the considered spin systems the ground-state degeneracy at saturation and therefore entropy can be calculated exactly by mapping the localized magnon problem onto a related lattice gas model of hard-core objects. The latter models have been studied in many papers over the last few decades (see Refs. 7,8,9,10 and references therein). We complete these analytical findings for the ground-state entropy by exact diagonalisation data for the sawtooth chain of $N = 8, 12, 16$ sites to extend our conclusions to fields below the saturation and to nonzero temperatures. We also examine the effects of exchange anisotropy, different spin values s and devia-

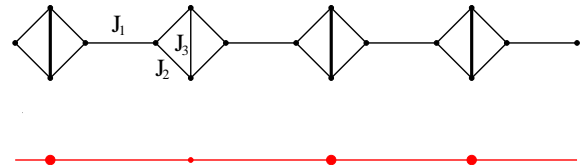


FIG. 1: The dimer-plaquette chain which hosts three localized magnons at fat bonds (top) and the auxiliary lattice used for the calculation of the ground-state degeneracy at saturation (bottom). The localized magnons are eigenstates for large enough vertical bonds $J_3 \geq J_3^c(J_1, J_2)$ ¹⁶.

tions from the condition on bond strengths under which the independent localized magnons are exact eigenstates for the sawtooth chain. Finally, we discuss briefly the possibility of experimental verification of our findings.

We mention recent papers of Moessner and Sondhi¹¹, Zhitomirsky¹² and Udagawa et al.¹³ having some relation to our investigations. These authors calculate the ground-state degeneracy of the 2D kagomé lattice carrying *classical* spins for certain spin configurations (up-up-down structure^{11,12} and structures obeying a “modified ice rule”¹³) by mapping the spin problem onto a dimer-covering problem on the honeycomb lattice. Udagawa et al. use their result to explain the residual entropy of the kagomé ice state which occurs in the spin ice compound $Dy_2Ti_2O_7$ under a magnetic field^{14,15}. Note, however, that our study refers to the frustrated *quantum* spin lattices.

To be specific, we consider several geometrically frustrated lattices, namely, the dimer-plaquette chain¹⁶ (Fig. 1), the sawtooth chain^{17,18} (Fig. 2), two kagomé-like chains^{19,20} (Figs. 3, 4), the kagomé lattice (Fig. 5), and the checkerboard (also called 2D or planar pyrochlore) lattice (Fig. 6). The ground-state and low-temperature properties for the Heisenberg antiferromagnet on these lattices are subjects of intensive discussions. We consider

*On leave of absence from the Institute for Condensed Matter Physics, National Academy of Sciences of Ukraine, 1 Svientsitskii Street, L'viv-11, 79011, Ukraine

†On leave of absence from Institut für Theoretische Physik, Universität Magdeburg, P.O. Box 4120, D-39016 Magdeburg, Germany

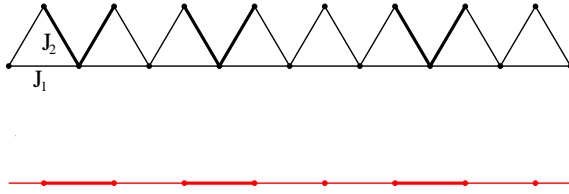


FIG. 2: The sawtooth chain which hosts three localized magnons at fat V parts (top) and the auxiliary lattice used for the calculation of the ground-state degeneracy at saturation (bottom). The localized magnons are eigenstates for $J_2 = \sqrt{2(1+\Delta)}J_1$ ^{4,5}.

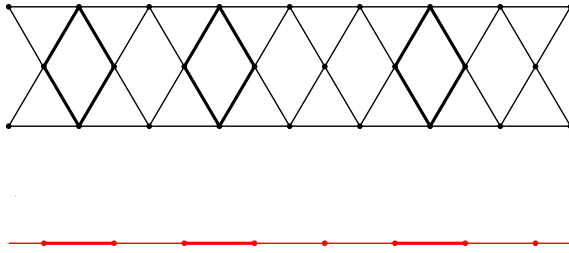


FIG. 3: The kagomé-like chain of Ref. 19 which hosts three localized magnons (marked by bold diamonds) and the auxiliary lattice used for the calculation of the ground-state degeneracy at saturation. The localized magnons are eigenstates for exchange bonds of uniform strength⁴.

N quantum spins of length s described by the Hamiltonian

$$H = \sum_{(nm)} J_{nm} (s_n^x s_m^x + s_n^y s_m^y + \Delta s_n^z s_m^z) - h \sum_n s_n^z \quad (1)$$

where the first sum runs over the bonds (edges) which connect the sites (vertices) occupied by spins for the mentioned lattices, $J_{nm} > 0$ is the antiferromagnetic exchange constant between neighboring sites, Δ is the anisotropy parameter, h is the external magnetic field, and the second sum runs over all sites. We know from Refs. 4,5, that for certain values of J_{nm} the considered lattices host localized magnons (see also the corresponding Figs. 1 – 6). Due to these localized magnons the ground state of (1) for the mentioned lattices at the saturation field h_1 is highly degenerate, since the energies of n independent localized magnon states with $n = 1, \dots, n_{\max}$, $n_{\max} \sim N$ are exactly the same. Because a certain local fragment of the lattice can be occupied by a magnon or not, the degeneracy of the ground state at saturation, \mathcal{W} , grows exponentially with N giving rise to a finite zero-temperature entropy per site at saturation

$$\frac{S}{k} = \lim_{N \rightarrow \infty} \frac{1}{N} \log \mathcal{W}. \quad (2)$$

The counting problem associated with the ground-state degeneracy can be solved after mapping the lattice which hosts independent localized magnons onto some auxiliary lattice which is occupied by hard-core objects

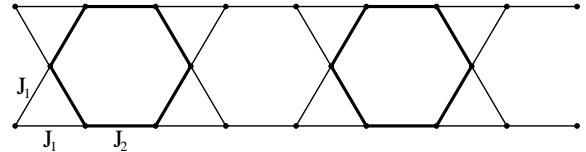


FIG. 4: The kagomé-like chain of Refs. 19,20 which hosts two localized magnons (marked by bold hexagons) and the auxiliary lattice used for the calculation of the ground-state degeneracy at saturation. The localized magnons are eigenstates for $J_2 = \frac{1+2\Delta}{1+\Delta} J_1$ ⁴.

(monomers, or monomers and dimers, or hexagons, or squares).

We start with the dimer-plaquette chain shown in Fig. 1. The auxiliary lattice (Fig. 1, bottom) is a linear chain of $\mathcal{N} = \frac{1}{4}N$ sites which may be either occupied (if a localized magnon is trapped by the corresponding fragment of the initial lattice) or empty (in the opposite case). Obviously,

$$\mathcal{W} = 2^{\mathcal{N}} = \exp \left(\frac{1}{4} \log 2 N \right) \approx \exp(0.173287N). \quad (3)$$

Repeating these arguments for the diamond chain²¹ we arrive at the similar result, $\mathcal{W} = 2^{\mathcal{N}}$, however, with $\mathcal{N} = \frac{1}{3}N$.

Next we consider the sawtooth chain shown in Fig. 2. The auxiliary chain (Fig. 2, bottom) consists of $\mathcal{N} = \frac{1}{2}N$ sites which may be filled either by rigid monomers or by rigid dimers occupying two neighboring sites. The limiting behavior of \mathcal{W} for a large lattice $\mathcal{N} \rightarrow \infty$ may be found in Ref. 7

$$\mathcal{W} = \exp \left(\log \frac{1 + \sqrt{5}}{2} \mathcal{N} \right) \approx \exp(0.240606N). \quad (4)$$

The same result (4) holds for the two-leg ladder of Refs. 22,23 (see Fig. 1a of Ref. 23). Similarly, for the kagomé-like chains shown in Figs. 3, 4 we get

$$\mathcal{W} = \exp \left(\frac{1}{3} \log \frac{1 + \sqrt{5}}{2} N \right) \approx \exp(0.160404N) \quad (5)$$

and

$$\mathcal{W} = \exp \left(\frac{1}{5} \log \frac{1 + \sqrt{5}}{2} N \right) \approx \exp(0.096242N), \quad (6)$$

correspondingly.

Let us pass to the 2D case. Considering the kagomé lattice (Fig. 5) we identify i) the centres of hexagons (which may trap magnons) as the sites of the auxiliary triangular lattice and ii) the hexagons carrying localized magnons together with the six attached triangles as the

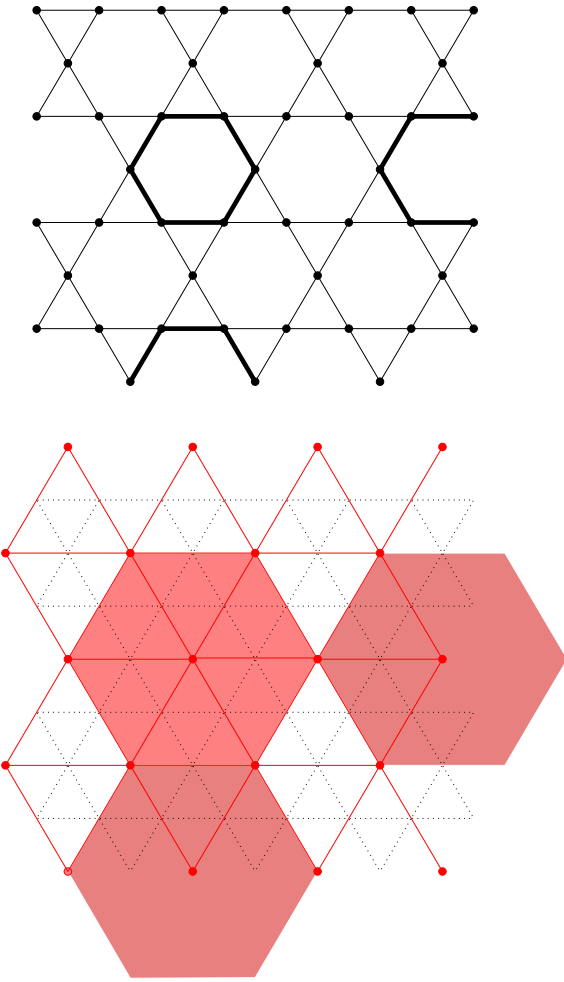


FIG. 5: The kagomé lattice which hosts three localized magnons (bold hexagons) and the auxiliary triangular lattice with hard hexagons used for the calculation of the ground-state degeneracy at saturation. The localized magnons are eigenstates for exchange bonds of uniform strength⁴.

shaded hexagons on the triangle lattice. Now it is evident that the filling of the kagomé lattice by localized magnons corresponds to the occupation of the auxiliary triangular lattice by hard hexagons. The hard-hexagon model (i.e. the triangular lattice gas with nearest-neighbor exclusion) has been exactly solved⁹. In particular, for the number of ways of putting hard hexagons on the triangular lattice of $\mathcal{N} \rightarrow \infty$ sites the accurate estimate is⁹ $\exp(0.333242721976\dots \mathcal{N})$. Therefore, taking into account the relation between the number of sites N of kagomé lattice and the number of sites \mathcal{N} of the auxiliary triangular lattice, $N = 3\mathcal{N}$, we get

$$\mathcal{W} \approx \exp(0.111081N). \quad (7)$$

It should be noted here that the hard-hexagon model also arises while calculating \mathcal{W} for the star lattice^{3,24}, however, in that case $N = 6\mathcal{N}$.

Finally we consider the checkerboard lattice shown in Fig. 6. The construction of an auxiliary lattice for the

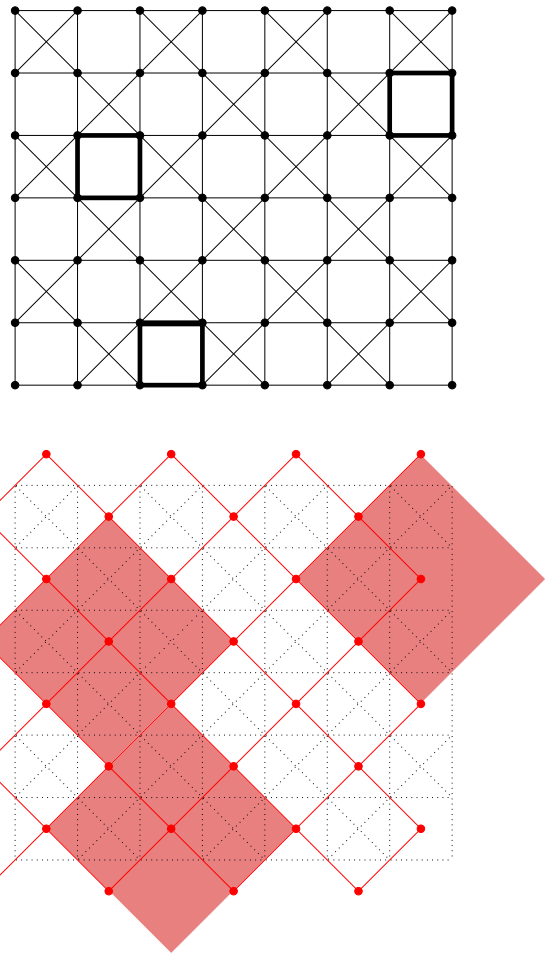


FIG. 6: The checkerboard lattice which hosts three localized magnons (bold squares) and the auxiliary square lattice with hard squares used for the estimation of the ground-state degeneracy at saturation. The localized magnons are eigenstates for exchange bonds of uniform strength⁵.

calculation of the ground-state degeneracy at saturation is illustrated in the lower part of Fig. 6. Each centre of the square which may host a localized magnon is represented by a site of the auxiliary square lattice. Moreover, the square hosting a magnon together with the eight attached triangles of the checkerboard lattice is represented by the shaded hard square (consisting of four elementary cells) of the auxiliary square lattice. A one-to-one correspondence between independent localized magnon configurations and shaded hard-square configuration obviously exists. As a result, we have to consider the square lattice gas with $\mathcal{N} = \frac{1}{2}N$ sites with nearest-neighbor and next-nearest-neighbor exclusion. We are not aware of an estimate of the entropy for such a model. (For the hard-square model (i.e. square lattice gas with only nearest-neighbor exclusion) the number of ways of putting hard squares on the square lattice of $\mathcal{N} \rightarrow \infty$ sites equals¹⁰ $\exp(1.503048082475\dots \mathcal{N})$.) A simple estimate for the lower bound for \mathcal{W} is $2^{\frac{N}{8}} \approx$

$$\exp(0.086643N).$$

To summarize this part, a class of frustrated quantum spin lattices has a huge degeneracy of the ground state at saturation that leads to a nonzero residual ground-state entropy. For some of such models the zero-temperature entropy at saturation $h = h_1$ can be estimated exactly. These values provide the “reference points” in the low-temperature dependence entropy S vs. field h for the corresponding lattices. It is remarkably that the calculation of \mathcal{W} is a pure combinatorial problem and therefore the values of the ground-state entropy at saturation are not sensitive to the value of anisotropy Δ or the value of spin s .

In what follows we discuss the dependence of the entropy S on the magnetic field h for $h < h_1$ at arbitrary temperatures using full exact diagonalisation of finite spin systems. We expect that the qualitative behavior is similar for all lattices considered. Here we focus on the sawtooth chain, because the ground-state degeneracy at saturation, \mathcal{W} , is largest and the finite-size effects should be smallest. We have considered sawtooth chains of $N = 8, 12, 16$ sites with $J_1 = 1$, $J_2 = \sqrt{2(1+\Delta)}$, anisotropy parameters $\Delta = 1$ and $\Delta = 0$, spin lengths $s = \frac{1}{2}, 1, \frac{3}{2}$ at several temperatures $kT = 0.001, 0.05, 0.2, 0.5, 1$. Some of our numerical results are shown in Figs. 7, 8.

Let us discuss the obtained results. Firstly we note that for several magnetic fields below saturation $h < h_1$ one has a two-fold or even a three-fold degeneracy of the energy levels leading in a finite system to a finite zero-temperature entropy. Correspondingly one finds in Fig. 7 (upper panel) a peaked structure and moreover a plateau just below saturation. However, it is clearly seen in Fig. 7 (upper panel) that the height of the peaks and of the plateau decreases with system size N and one has $S = 0$ at $T = 0$ as $N \rightarrow \infty$ for $h < h_1$ and $h > h_1$, only the peak at $h = h_1$ does not vanish. At finite temperatures this peak survives as a well-pronounced maximum and it only disappears if the temperature grows up to the order of the exchange constant, Fig. 7 (lower panel). The value of entropy at saturation, which agrees with the analytical prediction (4), is almost temperature independent up to about $kT \approx 0.2$, see Fig. 7. Moreover, the value of entropy at saturation is also almost size-independent as it follows from data for different N . Thus, the effect of the independent localized magnons which yield the residual ground-state entropy survives at finite temperatures $kT \lesssim 0.2$ producing a noticeable enhancement in the isothermal entropy curve at the saturation field.

By calculating results for $\Delta = 0$ and $\Delta = 1$ and for $s = 1, \frac{3}{2}$ and $s = \frac{1}{2}$ we have checked that the maximum in the entropy at saturation for low temperatures is robust against exchange interaction anisotropy and appears also for larger spin values s . However, our numerical results suggest that the enhancement of the entropy at saturation for finite temperatures becomes less pronounced with increasing s . A simple reason for that could be the circumstance that the degeneracy at saturation does not

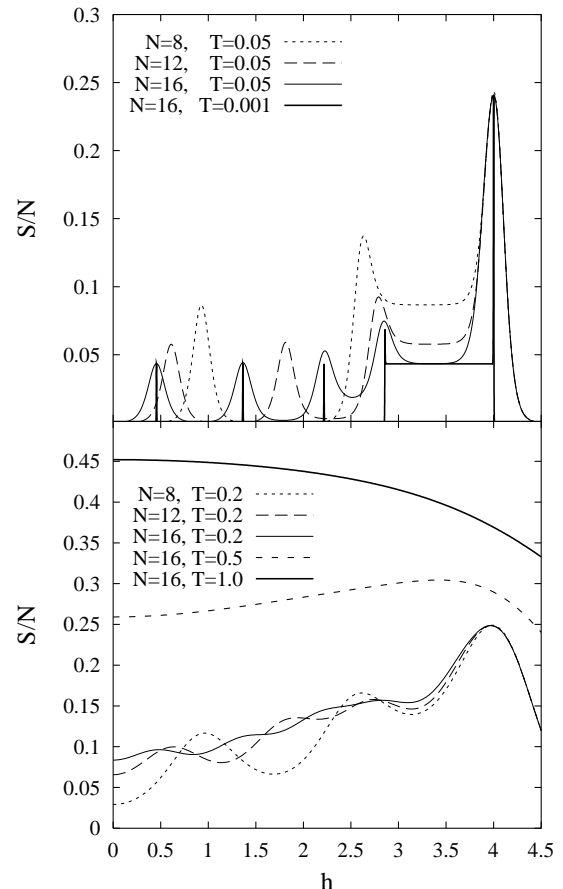


FIG. 7: Field dependence of the isothermal entropy per site at low temperatures (upper panel) and higher temperatures (lower panel) for the sawtooth chains of different length ($s = \frac{1}{2}, \Delta = 1, J_1 = 1, J_2 = 2$).

depend on spin value s , but the total number of state increases with s according to s^N .

Concerning the experimental confirmation of the predicted behavior of the entropy in real compounds we are faced with the situation that the conditions on bond strengths under which the independent localized magnons become the exact eigenstates^{3,4,5} are certainly not strictly fulfilled. For example, for the isotropic Heisenberg sawtooth chain (1) we have imposed $J_2 = 2J_1$, see Fig. 7. Therefore, it is useful to discuss the “stability” of our conclusions against deviation from the perfect condition for bond strengths. For this purpose we examine numerically the field dependence of entropy at low temperatures for the $s = \frac{1}{2}$ isotropic sawtooth chain of $N = 16$ sites with $J_1 = 1$ and $J_2 = 1.9$ and $J_2 = 2.1$ (Fig. 8). Evidently, the degeneracy of the ground state at saturation is lifted when $J_2 \neq 2$ that immediately yields zero entropy at saturation at very low temperatures (long-dashed and short-dashed curves in the upper panel of Fig. 8). However, the initially degenerate energy levels remain close to each other, if J_2 only slightly deviates from the perfect value 2. Therefore with in-

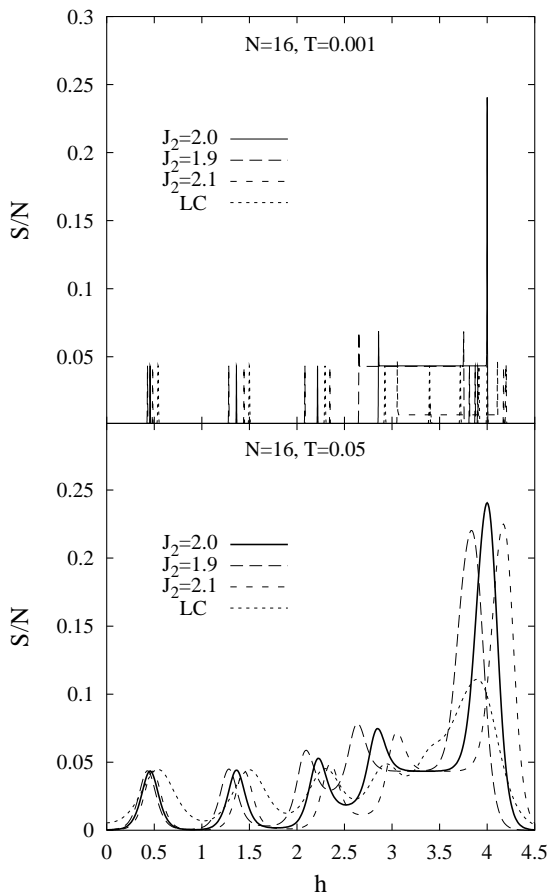


FIG. 8: Field dependence of the isothermal entropy per site of the sawtooth chain at very low temperature (upper panel) and at higher (but still low) temperature (lower panel) as J_2 deviates from $\sqrt{2}(1+\Delta)J_1$. The corresponding dependence for a linear chain (LC, dotted curves) is also reported for comparison.

creasing temperature those levels become accessible for the spin system and they manifest themselves in the entropy enhancement in the vicinity of saturation at low but nonzero temperatures. This can be nicely seen in the lower panel in Fig. 8 (long-dashed and short-dashed peaks in the vicinity of saturation). To demonstrate that this enhancement is the effect of the localized magnon states in the considered frustrated quantum spin lattice we also report the field-dependent entropy of the $s = \frac{1}{2}$ isotropic linear chain of $N = 16$ sites (dotted curves in Fig. 8) which remains in this field region at least two times smaller.

Let us remark that the ground-state degeneracy problem of antiferromagnetic Ising lattices in the critical magnetic field (i.e. at the spin-flop transition point), which obviously do not contain quantum fluctuations, has been discussed in the literature²⁵. Thus, the exactly solvable case of the antiferromagnetic Ising chain at critical magnetic field provides another example of the low-temperature entropy enhancement at saturation. From

Ref. 25 we know that at zero temperature $\mathcal{S} = k \log \frac{1+\sqrt{5}}{2}$ for $s = \frac{1}{2}$. Repeating the transfer matrix calculations for $s = 1$ and $s = \frac{3}{2}$ we find instead $\mathcal{S} = k \log 2$ and $\mathcal{S} = k \log \frac{1+\sqrt{13}}{2}$, respectively, that shows that the zero-temperature entropy at critical field depends on the spin value s . On the contrary, for the frustrated quantum spin lattices considered in the present paper the zero-temperature entropy at saturation does not depend on s .

Finally, we should emphasize that there are other lattices which support the independent localized magnon states e.g., the 2D square-kagomé lattice or the 3D pyrochlore lattice^{4,5}. In these cases a rigorous result for the ground-state degeneracy at saturation is not available, but for the existing huge degeneracy at saturation a lower bound is given by³ $\mathcal{W} \geq 2^{n_{\max}}$ where $n_{\max} \sim N$ is the maximum number of localized magnons which depends on the lattice geometry. This leads to the conclusion that the discussed low-temperature peculiarity of the entropy in the vicinity of saturation should also be present. Hence, the low-temperature maximum of \mathcal{S} at saturation is a generic effect for strongly frustrated quantum spin lattices which may host independent localized magnons.

From the experimental point of view the discussed effect of the independent localized magnons on the low-temperature field dependence of the entropy in the vicinity of saturation may be of great importance. Really, although the most spectacular effect of the independent localized magnons is a jump in the zero-temperature magnetisation curve just below the saturation^{3,4,5}, it is probably difficult to observe the jump at finite temperatures. The above discussed maximum in the entropy vs. field curve due to independent localized magnons is certainly easier accessible for experimental observation, since the isothermal entropy as a function of field can be obtained from a specific-heat measurement (see, e.g. Refs. 14,15). We also mention the significance of the maximum in the entropy vs. field curve to an enhanced magnetocaloric effect²⁶.

To summarize, we have rigorously calculated the finite ground-state entropy at the saturation field for some strongly frustrated quantum spin lattices hosting localized magnons. To discuss the physical relevance of these results we have examined the field dependence of entropy at low temperatures for these frustrated systems. We have found that the independent localized magnon states produce a maximum in the isothermal entropy versus field curve in the vicinity of the saturation field at low temperatures. This effect is robust against small deviations from the condition on bond strengths under which the localized magnons exist. The reported behavior can manifest itself in the high-field specific heat measurements permitting to detect experimentally the independent localized magnons in frustrated quantum spin lattices.

Acknowledgments: We would like to thank R. Moess-

ner and A. Honecker for fruitful discussions and J. Schulenburg for assistance in numerical calculations. We are in particular indebted to R. Moessner who brought our attention to the residual entropy calculation and the hard-hexagon problem. J. R. and O. D. acknowl-

edge the kind hospitality of the Max-Planck-Institut für Physik komplexer Systeme (Dresden) in the spring of 2004. This work was partly supported by the DFG (project Ri615/12-1).

¹ C. Lhuillier and G. Misguich, in “High Magnetic Fields: Applications in Condensed Matter Physics and Spectroscopy”, C. Berthier, L. P. Lévy and G. Martinez, Eds. (Lecture Notes in Physics, 595) (Springer, Berlin, 2002), pp.161-190; arXiv:cond-mat/0109146.

² G. Misguich and C. Lhuillier, arXiv:cond-mat/0310405.

³ J. Richter, J. Schulenburg, and A. Honecker, *Quantum magnetism in two dimensions: From semi-classical Néel order to magnetic disorder* [<http://www.tu-bs.de/~honecker/papers/2dqm.ps.gz>], in “Quantum Magnetism”, U. Schollwöck, J. Richter, D.J.J. Farnell and R. F. Bishop, Eds. (Lecture Notes in Physics) (Springer, Berlin, 2004), in press.

⁴ J. Schulenburg, A. Honecker, J. Schnack, J. Richter, and H. - J. Schmidt, Phys. Rev. Lett. **88**, 167207 (2002).

⁵ J. Richter, J. Schulenburg, A. Honecker, J. Schnack, and H. - J. Schmidt, J. Phys.: Condens. Matter **16**, S779 (2004).

⁶ J. Richter, O. Derzhko, and J. Schulenburg, arXiv:cond-mat/0312216.

⁷ M. E. Fisher, Phys. Rev. **124**, 1664 (1961).

⁸ R. J. Baxter, I. G. Enting, and S. K. Tsang, J. Stat. Phys. **22**, 465 (1980).

⁹ R. J. Baxter and S. K. Tsang, J. Phys. A **13**, 1023 (1980); R. J. Baxter, J. Phys. A **13**, L61 (1980); R. J. Baxter, Exactly Solved Models in Statistical Mechanics (Academic Press, London, 1982).

¹⁰ R. J. Baxter, Annals of Combinatorics **3**, 191 (1999); arXiv:cond-mat/9811264.

¹¹ R. Moessner and S. L. Sondhi, Phys. Rev. B **63**, 224401 (2001).

¹² M. E. Zhitomirsky, Phys. Rev. Lett. **88**, 057204 (2002).

¹³ M. Udagawa, M. Ogata, and Z. Hiroi, J. Phys. Soc. Jpn. **71**, 2365 (2002).

¹⁴ K. Matsuhira, Z. Hiroi, T. Tayama, S. Takagi, and T. Sakakibara, J. Phys.: Condens. Matter **14**, L559 (2002).

¹⁵ Z. Hiroi, K. Matsuhira, S. Takagi, T. Tayama, and T. Sakakibara, J. Phys. Soc. Jpn. **72**, 411 (2003).

¹⁶ N. B. Ivanov and J. Richter, Phys. Lett. A **232**, 308 (1997); J. Richter, N. B. Ivanov, and J. Schulenburg, J. Phys.: Condens. Matter **10**, 3635 (1998).

¹⁷ T. Nakamura and K. Kubo, Phys. Rev. B **53**, 6393 (1996).

¹⁸ D. Sen, B. S. Shastry, R. E. Walstedt, and R. Cava, Phys. Rev. B **53**, 6401 (1996).

¹⁹ Ch. Waldtmann, H. Kreutzmann, U. Schollwöck, K. Maisinger, and H. - U. Everts, Phys. Rev. B **62**, 9472 (2000).

²⁰ P. Azaria, C. Hooley, P. Lecheminant, and A. M. Tsvelik, Phys. Rev. Lett. **81**, 1694 (1998).

²¹ H. Niggemann, G. Uimin, and J. Zittartz, J. Phys.: Condens. Matter **9**, 9031 (1997).

²² F. Mila, Eur. Phys. J. B **6**, 201 (1998).

²³ A. Honecker, F. Mila, and M. Troyer, Eur. Phys. J. B **15**, 227 (2000).

²⁴ J. Richter, J. Schulenburg, A. Honecker, and D. Schmalfuß, in preparation.

²⁵ B. D. Metcalf and C. P. Yang, Phys. Rev. B **18**, 2304 (1978).

²⁶ M. E. Zhitomirsky, Phys. Rev. B **67**, 104421 (2003); M. E. Zhitomirsky and A. Honecker, in preparation.